SASEC
1st Southern African Solar Energy Conference
21-23 May 2012

A WIND LOADING CORRELATION FOR AN ISOLATED SQUARE HELIOSTAT PART 2: MOMENTS AND SIDE FORCES

Thomas H Roos[1]

[1] CSIR, P O Box 395, Pretoria, 0001, South Africa; Phone: +27 12 841-2329; Fax: +27 12 349-1156; E-Mail: throos@csir.co.za

Abstract

One of the design requirements of a heliostat is the ability to withstand storm wind loads in the stow position and operational wind loads in any position. To design a heliostat, therefore, one must be able to predict the wind loading on the heliostat for all elevation angles of the heliostat and all wind directions relative to the heliostat coordinate system. A companion paper has described a technique for using of Fourier analysis to fit a small number of correlations to a large experimental wind tunnel force and moment coefficient dataset for an isolated heliostat, and presented correlations for the lift and drag forces. In this paper correlations for the side forces and for moments about the three principal axes are presented, the behavior of the correlations is discussed and comparisons are made to recently published heliostat mean loading data.

Keywords: heliostat; wind; loading; correlation; Peterka

1. Introduction

One of the design requirements of a heliostat is the ability to withstand three types of wind loads [1]: 1) storm winds: in discrete, infrequent storm loads of up to 40m/s wind speed, heliostat in *stowed* position must survive (no static failure or low cycle fatigue failure); 2) moderate winds: at wind speeds up to 22m/s, a heliostat in *any* position must survive (no static failure or low cycle fatigue failure), and the actuation mechanisms must be able to move the heliostat to the stow position in preparation for possible storm winds; and 3) operational winds: at more frequent oscillating wind speeds up to 15m/s, the actuation mechanisms must be capable to allow a heliostat in *any* position to accurately track the sun, and the resultant loads should not lead to high cycle fatigue failure.

In the above, wind speeds are freestream values are measured at 10m above ground. To design a heliostat, therefore, one must be able to predict the mean and oscillating wind loads on the heliostat for all elevation angles of the heliostat and all wind directions relative to the heliostat coordinate system.

Peterka et al [2] performed wind tunnel tests on a 1/60th scale square isolated heliostat model placed in a dedicated atmospheric boundary layer wind tunnel. This data is useful, for several reasons. Firstly, it is an extensive and comprehensive dataset. Force and moment measurements were taken of the heliostat model at 6 heliostat setting angles (α = 0˚, 3˚, 6˚, 10˚, 45˚, 90˚) at 9 wind directions (θ = 0˚, 22.5˚, 45˚, 67.5˚, 90˚, 112.5˚, 135˚, 157.5˚ and 180˚) and at a further 4 heliostat setting angles (α = 15˚, 30˚, 60˚ and 75˚) at wind directions with coarser increments (θ = 0˚, 45˚, 90˚, 135˚, and 180˚). At each α and θ setting, 6 values (maximum, minimum, mean, RMS, peak factor ratio[1] and gust factor[2]) are given relating to the coefficients of the components of force and moment for each of the 3 principal directions (CF_x, CF_y, CF_z, CM_x, CM_y and CM_z). Secondly, it is in the public domain. Such a dataset would be very expensive to recreate, setting up a barrier to entry for researchers. Lastly, it is representative. Care was taken to reproduce the velocity and turbulence profiles appropriate for turbulent wind blowing over flat ground.

A companion paper to this one [3] describes the process of fitting appropriate correlations to this experimental dataset, to avoid having to interpolate within points in a large dataset. It is recommended that the companion paper be read first, but for convenience its contents will be briefly summarized. Firstly, details of the wind tunnel test series were described. Secondly, quality control was applied to the published

[1] $Pfact = (peak - mean)/RMS$
[2] $Gfact = peak/mean$

data: the non-dimensionalised force and moment data was published only to two decimal places, leading to unacceptably low resolution in many instances. The published *Pfact* and *Gfact* relationships (mentioned earlier) were exploited to regenerate the mean and RMS data values to more significant figures. Thirdly, a normal distribution of datapoints was assumed around each mean value, leading to the assumption that the maximum and minimum values lay at 4 RMS values from each mean value. This simplification means that only mean and RMS distributions need be correlated to recreate the maximum and minimum distributions. Finally, using Fourier analysis, correlations were created for the $CF_{x\ mean}$, $CF_{x\ RMS}$, $CF_{z\ mean}$ and $CF_{z\ RMS}$ distributions. This allows the recreation of maximum and minimum lift and drag forces.

In this paper, correlations will be developed for the side forces as well as for all moments. Taken together, this will allow a heliostat designer to develop reliable wind load data for the support structure and actuation systems for any heliostat.

The correlations will be compared to published wind load data for a commercially available heliostat.

2. Correlation curve fitting

2.1. Axis and sign convention

Figure 1 (left) shows the geometry of the 1/60th scale square isolated heliostat model used in the wind tunnel [2]. The sign convention[3] is that used by [2] and is illustrated in Figure 1 (right): the heliostat azimuth angle is measured anticlockwise from east and in all cases is 270˚ (y-axis runs due east, y-axis runs due south). The wind direction θ is measured clockwise from north (0˚) to south (180˚). While the heliostat elevation angle is measured from the vertical, in this paper this convention is replaced with angle of attack α, measured from horizontal (0° represents horizontal, 90° vertical).

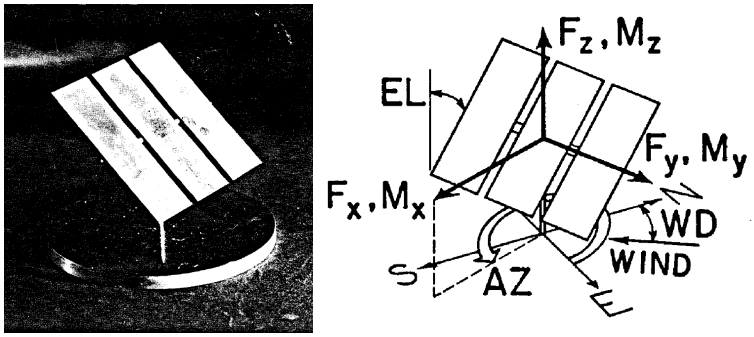

Figure 1: 1/60th scale heliostat (left), axis convention (right) [2]

2.2. $CF_{y\ mean}$

As can be seen in Figure 2, the $CF_{y\ mean}$ experimental curves resemble a negative sine function in wind angle (θ), with the magnitude showing very little dependence on heliostat setting angles (α), with maximum magnitude values approximately equal to 0.04 for all values of α except 90°. There is dependence on α for the curve shape, however: for α ≤ 10° the curves are approximately symmetrical about θ = 90°, and at higher values of α the shape is no longer symmetrical, with minimum values moving away from θ = 90° towards progressively smaller values of θ. It is surmised that this is due to the vertical heliostat pylon and the horizontal torque tube making the predominant symmetrical contribution to $CF_{y\ mean}$ at low α values through the mechanism of the drag of cylinders in crossflow, and the y-component of the lift and drag forces of the mirror array being small. At higher values of α, the mirror array plays a larger role: for θ < 90° the mirror array, pylon and torque tube all contribute, increasing the magnitude of $CF_{y\ mean}$ at these values of θ above those at lower α values. For θ > 90°, however, the horizontal torque tube and progressively more of the pylon lie in the wake of the mirror array, with the effect of the latter replacing that of the former, keeping the reducing the magnitude of $CF_{y\ mean}$ at these values of θ to those at lower α values.

Any correlation for $CF_{y\ mean}$ has to be an odd function, i.e. $f(-x) = -f(x)$, as wind from θ = -5° should

[3] This is given in [2], but is repeated here for the convenience of the reader.

induce a component of force parallel to the y-axis of the same magnitude but opposite sign as for wind from θ = 5°. This means that at θ = 0° the mean of that force component should be zero, so there can be no constant term in the correlation. A fit was obtained using:

$$CF_{y\,mean}(\alpha,\theta) = C_1(\alpha)\times \sin\theta + C_2(\alpha)\times \sin(2\theta)$$

C_1 and C_2 are correlated by the expressions:

0° ≤ α ≤ 75°: $C_1(\alpha) = -0.0419604$

75° < α ≤ 90°: $C_1(\alpha) = -0.0419604 + \frac{(\alpha-75)}{(90-75)}\times(-0.0721437 + 0.0419604)$

0° ≤ α ≤ 90°: $C_2(\alpha) = -9.8389E-04\times\alpha + 0.0062829$

2.3. $CF_{y\,RMS}$

$CF_{y\,RMS}$ follows a distribution resembling a sine function, (but being a RMS value is of course nett positive), but interestingly enough displays a dramatic asymmetry at θ = 90°. As in the case of $CF_{y\,mean}$, the correlation for $CF_{y\,RMS}$ has to be an even function. $CF_{y\,RMS}$ is correlated by:

$$CF_{y\,RMS}(\alpha,\theta) = C_3(\alpha)\times|\sin\theta| + C_4(\alpha) + C_5(\alpha,\theta)$$

The correlations fitted to C_3 and C_4 are:

$$C_3(\alpha) = -3.23685E-05\times\alpha + 0.00526496$$

$$C_4(\alpha) = 4.14055E-05\times\alpha + 0.00932223$$

0° ≤ α ≤ 75°: $C_5(\alpha,\theta) = 0$

75° < α ≤ 90°, 90° < θ ≤ 270°: $C_5(\alpha,\theta) = 0$

75° < α ≤ 90°, -90° < θ ≤ 90°: $C_5(\alpha,\theta) = 0 + \frac{(\alpha-75)}{(90-75)}\times(0.015 - 0)$

Using the previously calculated values of $CF_{y\,mean}$ and assuming $Pfact = 4$, values of $CF_{y\,max}$ and $CF_{y\,min}$ as a function of wind angle θ and elevation angle α can be calculated from

$$CF_{y\,max}(\alpha,\theta) = CF_{y\,mean}(\alpha,\theta) + 4\times CF_{y\,RMS}(\alpha,\theta)$$

$$CF_{y\,min}(\alpha,\theta) = CF_{y\,mean}(\alpha,\theta) - 4\times CF_{y\,RMS}(\alpha,\theta)$$

2.4. $CM_{x\,mean}$

T-design or conventional heliostats are actuated around the z-azis (azimuth drive) and y-axis (elevation drive). Therefore wind-induced moments around the x-axis (CM_x) are of concern for the designer of such heliostats only for structural rather than actuation reasons. The two orthogonal degrees of freedom of target-aligned heliostats, however, do not coincide with the x-, y- and z-axes as a rule. For this reason CM_x is of interest for actuation calculations of target-aligned heliostats.

The shape (rather than the magnitude) of the experimental curves of $CM_{x\,mean}$ that show a noticeable dependence on α. The dominant shape is that of cos 2θ, with other harmonics varying a subordinate role. Like $CF_{y\,mean}$, the correlation for $CM_{x\,mean}$ has to be an odd function, leading to the following fit:

$$CM_{y\,mean}(\alpha,\theta) = C_6(\alpha)\times \sin\theta + C_7(\alpha)\times \sin(2\theta) +$$

$$C_8(\alpha)\times \sin(3\theta) + C_9(\alpha)\times \sin(4\theta)$$

Except for C_7 for values of α between 10° and 60°, C_6 to C_9 are correlated by linear interpolations between values at discrete α points given in Table 1, otherwise:

10° ≤ α ≤ 60°: $C_7(\alpha) = 1.79242E-06\times\alpha^2 - 1.20037E-04\times\alpha + 0.00761863$

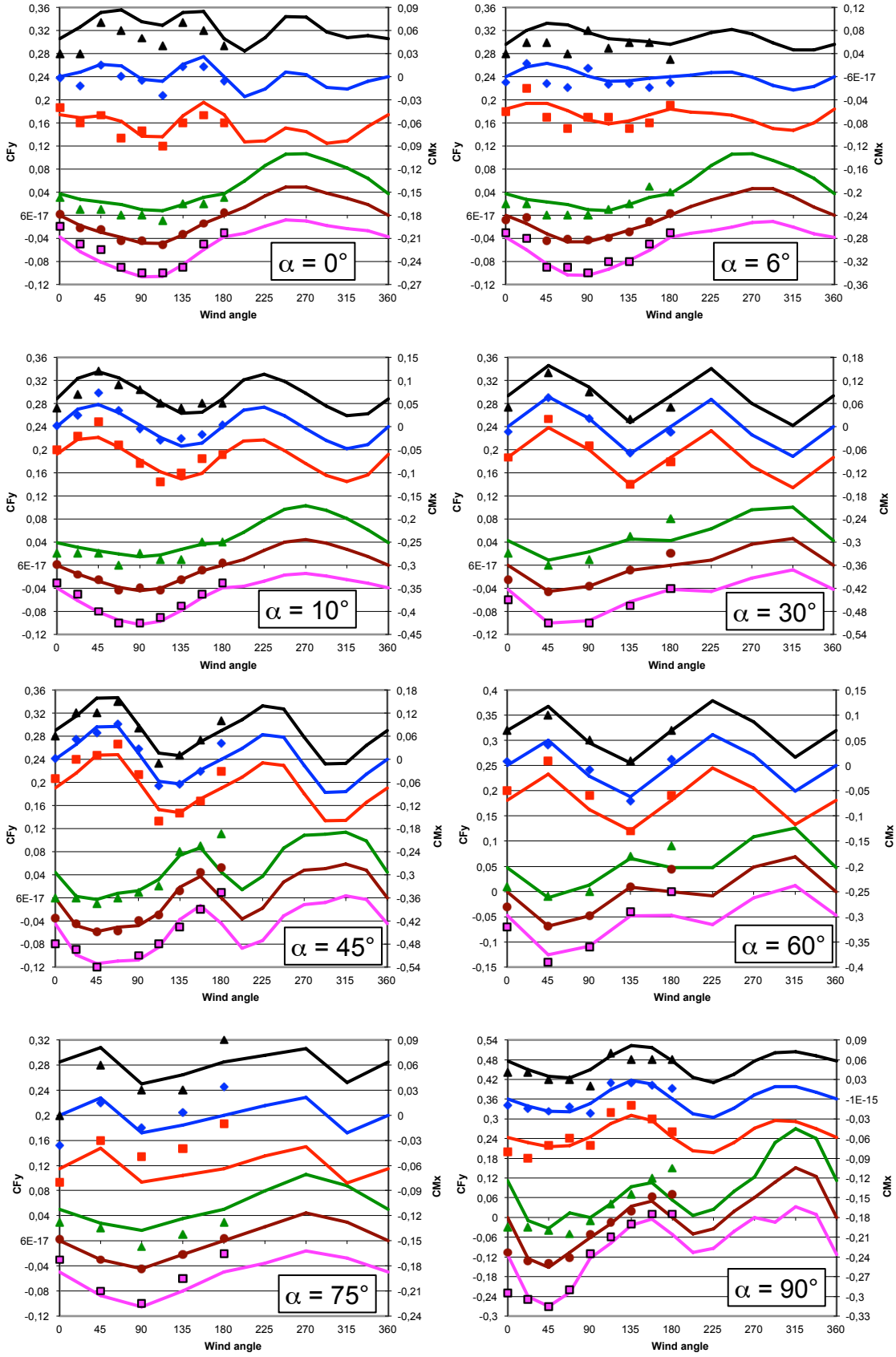

Figure 2: Comparison of data (markers) and correlation (lines) for CF_y min, mean and max (bottom 3 in each chart) and CM_x min, mean and max (top 3 in each chart) plotted versus □, for 8 values of □

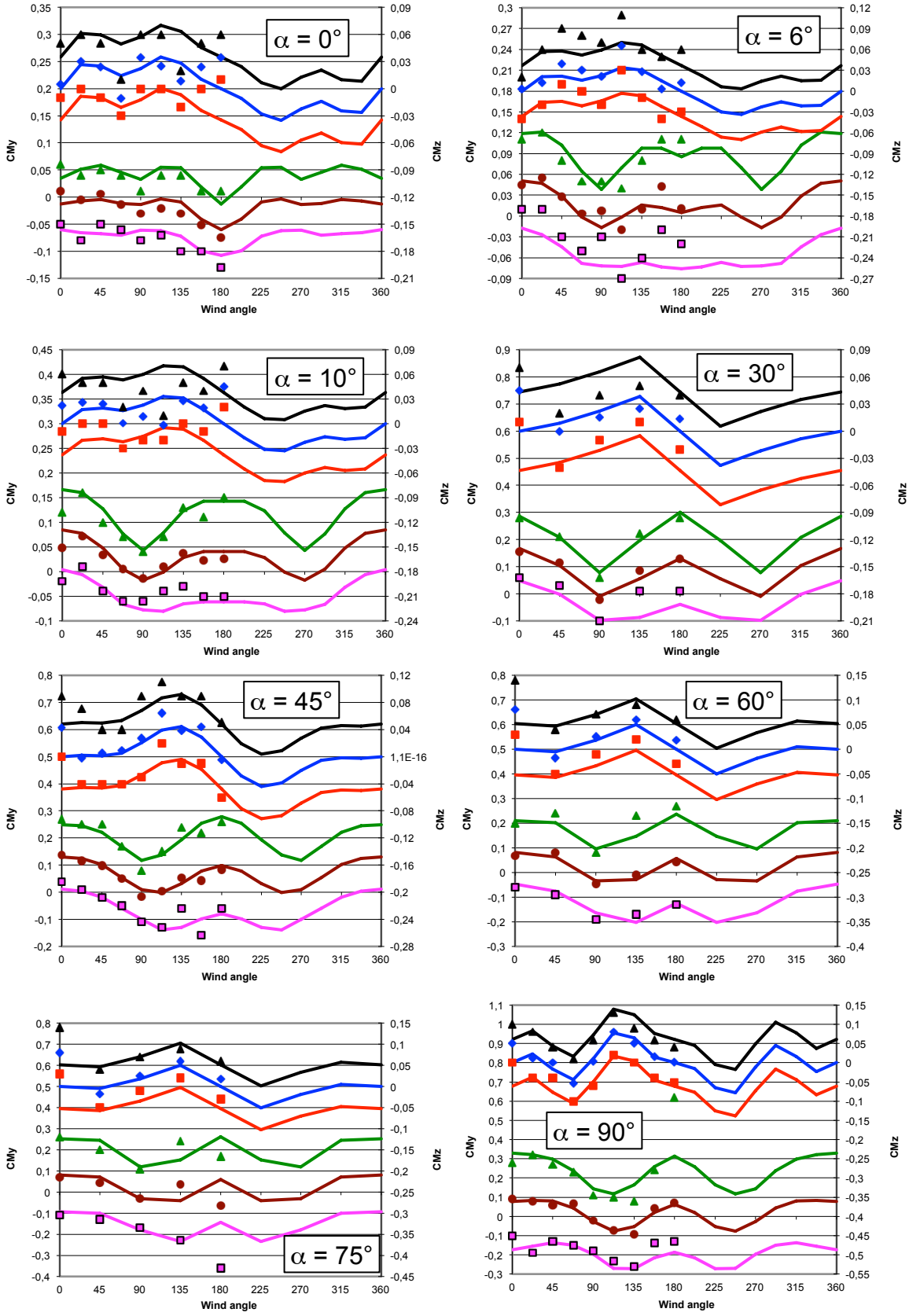

Figure 3: Comparison of data (markers) and correlation (lines) for CM_y min, mean and max (bottom 3 in each chart) and CM_z min, mean and max (top 3 in each chart) plotted versus □, for 8 values of □

Angle(°)	C_6	C_7	C_8	C_9	C_{10}	C_{11}
0	0.01	0	0.013	-0.01	0.00613214	-0.0123994
6	-	0.015	-	-	-	-
10	-	0.045	-	0.005	-	-
15	0.00094046	Polynomial	-	-	-	-
20	-	Polynomial	-0.013	-	-	-
30	0.0133604	Polynomial	-	-	0.00012789	0.0201218
45	0.014976	Polynomial	-	-0.019281	-	-
60	-0.014684	0.056073	-	-	-	-
75	-	-	0.0137394	-	-	-
90	0	-0.023518	0.0066125	0	-0.00183109	0.0146017

Table 1: Interpolation points for C_6 to C_{11}

2.5. $CM_{x\ RMS}$

$CM_{x\ RMS}$ follows a distribution resembling a nett positive sine function, similarly to $CF_{y\ RMS}$, leading to a similar correlation:

$$CF_{y\ RMS}(\alpha,\theta) = C_{10}(\alpha)\times|\sin\theta| + C_{11}(\alpha)$$

C_{10} to C_{11} are correlated by linear interpolations between values at discrete α points given in Table 1.

Using the $CM_{z\ RMS}$ and $CM_{z\ mean}$ correlations, and assuming $Pfact = 4$, values of $CM_{z\ max}$ and $CM_{z\ min}$ as a function of wind angle θ and elevation angle α can be calculated in the same manner as $CF_{y\ max}$ and $CF_{y\ min}$ values were calculated in section 2.3.

2.6. $CM_{y\ mean}$

A correlation for the moment around the y-axis (elevation or overturning moment CM_y) has to be an even function, i.e. $f(-x) = f(x)$, as wind from θ = -5° should induce the same moment about the y-axis as wind from θ = 5°. Constants are therefore allowed. A fit was obtained using:

$$CM_{y\ mean}(\alpha,\theta) = C_{12}(\alpha)\times\cos\theta + C_{13}(\alpha)\times\cos(2\theta) +$$
$$C_{14}(\alpha)\times\cos(3\theta) + C_{15}(\alpha)\times\cos(4\theta) + C_{16}(\alpha)$$

C_{12} to C_{16} are correlated by the expressions:

$0° \le \alpha \le 90°$: $C_{12}(\alpha) = 4.2094E-04\times\alpha + 0.0135797$

$0° < \alpha \le 45°$: $C_{13}(\alpha) = -1.06277\text{E}-04\times\alpha^2 + 6.20776\times\alpha - 0.011231$

$45° < \alpha \le 90°$: $C_{13}(\alpha) = 0.052907 + \frac{(\alpha-45)}{(90-45)}\times(0.048853 - 0.052907)$

$0° \le \alpha \le 90°$: $C_{14}(\alpha) = -6.02852E-04\times\alpha + 0.010301$

$0° \le \alpha \le 90°$: $C_{15}(\alpha) = 1.51916E-04\times\alpha - 0.009340$

$0° < \alpha \le 60°$: $C_{16}(\alpha) = -8.13822\text{E}-05\ \alpha^2 + 0.0054421\times\alpha - 0.015817$

$60° < \alpha \le 90°$: $C_{16}(\alpha) = 0.017732 + \frac{(\alpha-60)}{(90-60)}\times(0.017607 - 0.017732)$

2.7. $CM_{y\ RMS}$

As in the case of $CM_{y\ mean}$, the correlation for $CM_{y\ RMS}$ has to be an even function. The experimental $CM_{y\ RMS}$ curves have a similar shape to the $CF_{z\ RMS}$ curves [], so are therefore correlated by a similar function:

$$CM_{y\,RMS}(\alpha,\theta) = C_{17}(\alpha)\times|\sin(2\theta)| + C_{18}(\alpha)\times|\cos\theta| + C_{19}(\alpha)\times\cos\theta + C_{20}(\alpha)$$

The correlations fitted to C_{17} to C_{20} are:

$$C_{17}(\alpha) = -0.00324567\times\sin(4\alpha) - 7.0929E-05\times\alpha + 0.00399465$$

$$C_{18}(\alpha) = 0.00833605\times\sin(4\alpha) + 0.000221721\times\alpha + 0.00018968$$

$$C_{19}(\alpha) = -0.00751985\times\sin(2\alpha)$$

$$C_{20}(\alpha) = 0.00034340\times\alpha - 0.011678$$

Using the previously calculated values of $CM_{y\,mean}$ and assuming $Pfact = 4$, values of $CM_{y\,max}$ and $CM_{y\,min}$ as a function of wind angle θ and elevation angle α can be calculated in the same manner as $CF_{y\,max}$ and $CF_{y\,min}$ values were calculated in section 2.3.

2.8. $CM_{z\,mean}$

Unlike $CM_{y\,mean}$, any correlation for the moment around the z-axis (azimuth or pylon moment) $CM_{z\,mean}$ has to be an odd function, i.e. $f(-x) = -f(x)$, as wind from θ = -5° should induce a moment of the same magnitude but of opposite sign about the z-axis as wind from θ = 5°. This means that at θ = 0° the moment must be zero, so there can be no constant in the correlation. A fit was obtained using:

$$CM_{y\,mean}(\alpha,\theta) = C_{21}(\alpha)\times\sin\theta + C_{22}(\alpha)\times\sin(2\theta) +$$

$$C_{23}(\alpha)\times\sin(3\theta) + C_{24}(\alpha)\times\sin(4\theta)$$

The correlations fitted to C_{21} to C_{24} are:

$$C_{21}(\alpha) = -7.77774E-05\times\alpha + 0.029897$$

$$C_{22}(\alpha) = -4.33771E-04\times\alpha - 0.00170629$$

$$C_{23}(\alpha) = 1.79242E-06\times\alpha^2 - 1.20037E-04\times\alpha + 0.00761863$$

$$C_{24}(\alpha) = 9.36730E-06\times\alpha^2 - 5.84094E-04\times\alpha + 0.00917254$$

2.9. $CM_{z\,RMS}$

The $CM_{z\,RMS}$ curves display a definite dependency on heliostat setting angle α, but no discernable dependency on wind angle θ. For this reason they were regarded as constant at each value of α, simplifying the correlation:

$$CM_{z\,RMS}(\alpha,\theta) = 7.18803E-05\times\alpha + 0.00871019$$

Using the $CM_{z\,RMS}$ and $CM_{z\,mean}$ correlations, and assuming $Pfact = 4$, values of $CM_{z\,max}$ and $CM_{z\,min}$ as a function of wind angle θ and elevation angle α can be calculated in the same manner as $CF_{y\,max}$ and $CF_{y\,min}$ values were calculated in section 2.3.

3. Discussion

Examining all the predicted curves (not just those displayed in Figure 3), the $CF_{y\,mean}$ correlation displays is a excellent fit, only showing disagreement with experimental data at θ = 0° and θ = 180° for α values of 30° and above, where the requirement to be an odd function forces the value to be zero. Non-zero experimental values here cannot easily be explained. The $CF_{y\,max}$ and $CF_{y\,min}$ correlations similarly have excellent or conservative fits, again except at θ = 0° and θ = 180° for various values of α, and at θ = 45° at α = 60°.

The $CM_{x\,mean}$ correlation displays an excellent or conservative fit at α values between 30° and 75°, except for some non-zero experimental values at θ = 0° and θ = 180° for this odd function. At α = 6° and below the fit deteriorates, as no clear pattern is discernable that gives rise to a smooth correlation. The $CM_{x\,max}$ and $CM_{x\,min}$ correlations track the data well and will bound all the data if the Pfact value is increased slightly.

The $CM_{y\,mean}$ correlation displays a good fit except at α below 10° and at 75°. The $CM_{x\,max}$ and $CM_{x\,min}$

correlations track the data well and bound all the data except at and θ = 180° for α = 90° and α = 75° (both outliers due to Pfact values of 8.49 and 5.21 respectively instead of 4), at α = 45° and θ = 157.5°, at α = 6° and θ = 112.5° ($CM_{x\ min}$), θ = 157.5° and 180° (both $CM_{x\ max}$) and at α = 0° for nearly all $CM_{x\ min}$. not 4. The low-α problems would be solved by increasing Pfact slightly.

The odd functions $CM_{z\ mean}$, $CM_{z\ max}$ and $CM_{z\ min}$ correlations are all good fit at α values above 45°, except at θ = 0°. At α = 45°, the trend is good, but both $CM_{z\ mean}$ and $CM_{z\ max}$ underpredict some values. Increasing Pfact slightly will solve the $CM_{z\ max}$ underprediction, except at θ = 0° where the experiment defies the odd function theory anyway. At α values below 45° the $CM_{z\ mean}$ trend is reasonable, and $CM_{z\ max}$ and $CM_{z\ min}$ correlations bound the data (except at the θ = 0° and θ = 180°), except at α = 6°, where increasing Pfact slightly will relieve but not solve the underprediction.

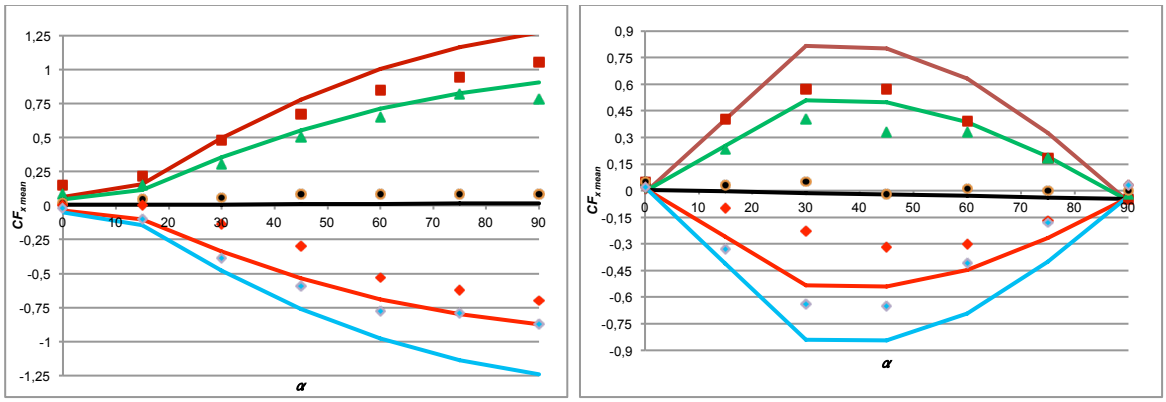

Figure 4: Comparison of data of Huss et al [4] (markers) and correlation (lines) for CF_x (left) and CF_z (right) as function of □ for □ values of 0° (brown), 60° (green), 90° (black), 120° (red) and 180° (blue)

Figure 4 shows a comparison of the wind tunnel data of Huss et al [4] for a low-aspect ratio, two-panel heliostat with the correlation for mean values of CF_x and CF_z. It can be seen that the low-aspect ratio follows the same trends as the square heliostat, but with lower absolute values.

4. Conclusion

Correlations for wind-induced side forces and moments have been presented and shown to have good fit for mean values, and maximum and minimum values tracking and largely bracketing all the data. Better bracketing will be achieved if Pfact values greater than 4 are used. Used together with the lift and drag force correlations presented in the companion paper [3], these should prove useful to heliostat designers.

Acknowledgements

The author would like to thank CSIR R&D office for directly supporting this work.

References

[1] Strachan J. W. and Houser R. M. (1993), "Testing and Evaluation of Large-Area Heliostats for Solar Thermal Applications", Sandia Laboratories Report SAND92-1381

[2] Peterka J.A., Hosoya N., Bienkiewicz B. and Cermak J. E., (1986), "Wind Load Reduction for Heliostats", Solar Energy Research Institute Subcontract Report for the U.S. Department of Energy, SERI/STR-253-2859, May 1986

[3] Roos T. H., (2012), "A Wind Loading Correlation For An Isolated Square Heliostat, Part 1: Lift And Drag Forces", Submitted to 1st SASEC, Stellenbosch, South Africa, 21-23 May 2012

[4] Huss S., Traeger Y.D., Shvets Z., Rojansky M., Stoyanoff S. and Garber J., (2011), "Evaluating Effects of Wind Loads in Heliostat Design", Proceedings of SolarPACES2011, Granada, Spain, September 2011